IEEE Access
Multidisciplinary | Rapid Review | Open Access Journal

Received December 29, 2019, accepted January 12, 2020, date of publication January 22, 2020, date of current version January 29, 2020.

*Digital Object Identifier 10.1109/ACCESS.2020.2968744*

# Data-Driven Feature Extraction for Analog Circuit Fault Diagnosis Using 1-D Convolutional Neural Network

**HUAHUI YANG, CHEN MENG, AND CHENG WANG**
Measurement Engineering Department, Army Engineering University, Shijiazhuang 050003, China
Corresponding authors: Huahui Yang (yanghh19@hotmail.com) and Cheng Wang (wangch11203@outlook.com)

This work was supported in part by the National Natural Science Foundation of China under Grant 61501493.

**ABSTRACT** The present study applies the one-dimensional convolutional neural network (1D-CNN) to propose an intelligent approach of the feature extraction for the analog circuit diagnosis. The raw signals based on various soft faults from the output terminal of the circuit under test (CUT) are collected with appropriate data acquisition system to implement a data-driven fault diagnosis. The data-driven diagnosis process is typically encapsulated in two distinct blocks, including the feature extraction and the classification. In this study, the designed 1D-CNN model efficiently combines the aforementioned two phases into a single diagnosis body with fast learning rate and accurate classification. The main advantages of the 1D-CNN are: 1) it can be directly established to the raw signal with proper training so that it is more applicable in real applications; 2) its compact architecture and configuration has reasonable applicability in complex analog circuits; 3) convolutional kernels guarantee that the hierarchical features can be extracted from raw data with better anti-interference performance. Moreover, since the method can extract high-level features of raw signals, it resolves the necessity to employ other per-processing methods for the hand-crafted feature transformation. The performance of the proposed 1D-CNN model is evaluated through three benchmark circuits on the SIMULINK platform. Obtained results are compared with other intelligent fault diagnosis methods. The experimental results show that the 1D-CNN can be utilized effectively as the feature exactor and faults classifier for analog circuits.

**INDEX TERMS** Analog circuit fault diagnosis, convolutional neural network, data-driven method, faults classification, feature extraction.

## I. INTRODUCTION

With high integration and wide application of analog circuits in modern electronic systems, the fault diagnosis of analog circuits has become a fundamental issue to perform reasonable maintenance and maintain the reliable operation of the system. Reviewing the literature shows that it has attracted much attention and achieved great research results since 1970s [1], [2]. Analogue circuits are more susceptible to interference and limited in test nodes. Moreover, analogue circuits have poor performance of component tolerance, and have more complex and complicated fault diagnosis system compared to digital circuits [3]. Moreover, less than 20% of analog circuits are responsible for more than 80% circuit faults [4]. Therefore, it is extremely essential to develop an effective fault diagnosis approach in electronic system health monitoring. This is more pronounced for soft faults, which mainly refer to abnormal variation of resistance, capacitance and inductance parameters. It should be indicated that power supply fluctuations, intense electromagnetic interference and poor solder joint contact are typical reasons of soft faults. Comparatively, hard faults in analog circuits would directly lead to catastrophic failures and are easier to be detected when the output of the circuit system seriously distorted [5]. To this end, it is still a challenging task to implement component-level diagnosis of the soft fault.

Analog circuit diagnosis approaches can be roughly divided into the modeling approaches and the data-driven approaches. The model-based methods mainly utilize measured signal responses under various conditions and outputs

The associate editor coordinating the review of this manuscript and approving it for publication was Yanzheng Zhu.

of circuit-model so that they are also known as signal-model methods. Liu *et al.* [6] combined a signal characterization model containing a feature extraction with the fault coding method to implement diagnostics and prognostics. Chen *et al.* [7] proposed an improved simulation-based multi-signal modeling for hard (F-fault and G-fault) and parametric faults. However, in this method, the Monte-Carlo simulation is determined explicitly and an adaptive threshold estimation is required. Other modeling approaches, including the matrix model [8], fuzzy model [9], parity space-based model [10] and the hidden Markov model (HMM) [11], are also combined with various signal processing methods for the fault diagnosis in analog circuits. Yang *et al.* [12] proposed a float encoding genetic algorithm that can model all parameter shifting faults with the grouped crossover, mutation and an integrated selection strategy. Moreover, the analytical ideas were adopted in the model-based approaches to establish the relationship of cause-effect dependency, such as the directed graph, decision trees, and fault dictionary methods, between the test and fault [13]. In summary, even in complex methods, the most fundamental principle of model-based approaches is to derive available transfer function equations for the analog circuit [14], [15]. For instance, a complex filed-based fault modeling is derived from the binary quadratic function that can characterize any continuous parameter shifting (soft) faults [16]. However, the modeling approaches require manual analysis and a great deal of prior knowledge. Furthermore, the modeling verification is extremely necessary and important for these models. Although these models have achieved great research results, it is a challenge to complete the fault diagnosis task with an unsupervised way. This is more pronounced for complex electronic systems.

Since establishment of modeling approaches is a great challenge, data-driven approaches have become more popular as they combine feature extraction and classification techniques into a single learning body. Reviewing the literature indicates that commonly used data-driven approaches are the artificial neural network (ANN) [17]–[22], support vector machine (SVM) [23], [24], and other machine learning methods [27], [28]. Zhao *et al.* [17] proposed an intelligent solution based on the deep belief network (DBN), which has higher classification accuracy and lower requirements on data. Similarly, Zhang *et al.* [4] adopted the DBN method for the feature extraction. However, the quantum-behaved particle swarm optimization (QPSO) is used to optimize the structure parameters of the DBN. Afterward, SVM benefiting from QPSO served as a classifier for incipient faults. The neural network has superior advantages in feature extraction and it is commonly combined with some signal preprocessing methods. For example, Gan *et al.* [20] presented a wavelet neural network (WNN), which is trained by a modified unscented Kalman filter (UKF) algorithm. Moreover, the wavelet transform and kernel linear discriminant analysis (KLDA), kurtosis and entropy of signals, and the maximal class separability based on kernel principal components analysis (MCSKPCA) are used as preprocessors in Ref. [19], [28] and [18], respectively. Furthermore, a multi-class adaptive neuro fuzzy interface system (ANFIS) is proposed in Ref. [22], which incorporates both ANN and fuzzy logic systems. Tan *et al.* [29] presented a systematic method, which combines neural networks and the genetic algorithm. Moreover, the SVM has been successfully applied in the fault diagnosis by using some signal transformation techniques as the preprocessor. For instance, in [30] and [31], SVDD based on the fractional wavelet transform (FTW) and improved LLSVR based on the nonlinear independent component analysis (NICA) are proposed, respectively. It should be indicated that the signal processing methods (NICA or FTW) are used for the feature extraction, while the latter methods (LLSVR or SVDD) are applied for the classification. Yuan *et al.* [32] used an improved hybrid particle swarm optimization (IH-PSO) algorithm to tune SVM parameters so that they achieved significant improvements in the initialization, convergence speed and the mechanism.

Considering the foregoing literature review, the most important advantages of data-driven approaches in the analog circuit fault diagnosis can be summarized as the following:

- The diagnosis model is established based on the artificial intelligence tools by automatic training.
- Classification results for faults can be autonomously obtained with implicit feature patterns discovered from a large number of historical data.
- This approach can also be combined with many statistical analysis methods and optimization algorithms to get better performances.

However, the data-driven diagnosis method still needs to extract features of underlying signals. On the other hand, the majority of performed investigations so far have been focused on fixed and manual feature extraction methods. Generally, these methods are along with the domain transformation that can significantly decrease the efficiency of algorithms. Furthermore, handcrafted features extracted by the preprocessing algorithm cannot represent deep characteristics of signals for different circuits. Meanwhile, these features can be hardly generalized in other applications [33]. In order to resolve these shortcomings, a compact 1D convolutional neural network (1D-CNN) is considered for analog circuit fault diagnosis with an automatic feature extraction process. A deep CNN model has a hierarchical neural network framework, in which the convolutional layers are employed as feature maps to achieve ''deep learning'' of features. Compared with conventional schemes, a simple 1D-CNN model achieves a superior performance in feature extraction and classification with limited training data. Moreover, filter kernels of the 1D-CNN can be optimized with proper training by a few dozens of back-propagation (BP) epochs so that it is an appropriate choice for processing one-dimensional signals. It should be indicated that in the present study, obtained results will be evaluated in three benchmark circuits.

The rest of this study is organized as follows: The architecture and detailed configuration of the 1D-CNN model is introduced in section 2. Fault diagnosis simulations based on

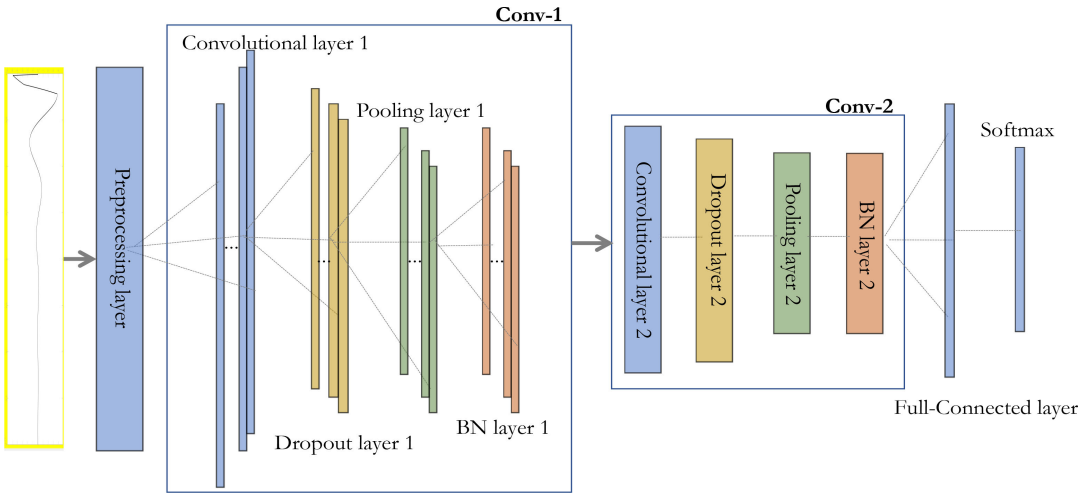


**FIGURE 1.** Architecture of the proposed adaptive 1D-CNN model.

three typical circuits are conducted to demonstrate the performance of 1D-CNN in section 3. Finally, main achievements and conclusions are presented in section 4.

## II. INTELLIGENT 1D-CNN METHOD FOR ANALOG CIRCUIT FAULT DIAGNOSIS

Reviewing the literature indicates that CNNs have reasonable performance in many pattern recognitions, such as the nature language processing [35], image classification [36] and the object detection in scene [37]. By applying the convolutional operation, CNNs construct a series of mapping to generate a succession of higher abstraction of input data, where each feature map can be called a channel and a convolutional operation filter. In the studied case, 1D-CNN which is sensitive to the one-dimensional time sequence, has been successfully applied in the electroencephalogram (EEG) and electrocardiogram (ECG) classification [38], [39], bearing and hydroelectric generating unit fault diagnosis [40], and the wheelset bearing fault diagnosis [41]. In a 2D-CNN model, input images are decimated to the class vectors at output layer. Hence, the entire configuration of the CNN model should be designed properly. In this regard, the topology of 1D-CNN model needs rational arrangements and certain modifications to perform the 1D (time-series) signal processing.

### A. OVERALL ARCHITECTURE

1D-CNN is utilized to process time series data in one dimensional form with convolutional (Conv) 1D layer, dropout layer, pooling (PL) 1D layer, batch normalization (BN) layer and fully connected (FC) layer and softmax classifier. Figure 1 illustrates the architecture of the proposed 1D-CNN model following an end-to-end diagnosis strategy without manual feature extraction procedure.

The architecture of compact CNNs is adaptive to process the input sequences of any dimension. Meanwhile, it is necessary to obtain the given output dimension of the last CNN layer by automatically assigning the sub-sampling factor of the last SS layer. This factor is set in accordance with the size of the practical input and objective output array. Figure 1 indicates that the sub-sampling factor of PL-2 layer in Conv-2 block can be adapted automatically so that the given output of this layer ca be set to an arbitrary dimension. Because of this "adaptive" design, the proposed 1D-CNN model has adaptation ability to set a proper number of CNN layers depending on the dimension of input signals.

Obviously, the convolution kernels and feature maps in 1D-CNN is a 1D-sequence instead of 2D matrices. Accordingly, the kernel size parameters and SS size are scalars, which are two major factors for 1D-CNN performance. Architectures and parameters should be set properly in accordance with various feature extraction and classification tasks for different circuits. Moreover, a dropout layer is added after the Conv layer to avoid overfitting, which is caused by increasing the model parameters with limited supervised learning. Since the distribution of feature maps changes during the training process, the BN layer is introduced to provide faster convergence and avoid special initialization of parameters [42]. There are two parameters of the BN layer, $\gamma$ and $\beta$, that should be iteratively updated by BP. It should be indicated that in the 1D-CNN model, the sum of parameters $\gamma$ and $\beta$ that shows acceptable number of parameters, is equal to $2 \times f_{\text{map length}} \times f_{\text{map num}}$,, which is much less than that of the 2D-CNN model.. Thanks to the BN layer, the "gradient diffusion" can be effectively prevented hence the convergence performance is improved with higher learning rate and lower dependency on the initialization of weights.

Eventually, a FC layer accompanied by a softmax classifier is applied for the signal classification, where higher features are extracted from upper layers. All CNN units in BN layers of *Conv* block are connected to each neuron of FC layer. By this compact design, the number of hidden *Conv* blocks can be set automatically for adapting to various fault classification in analog circuits.

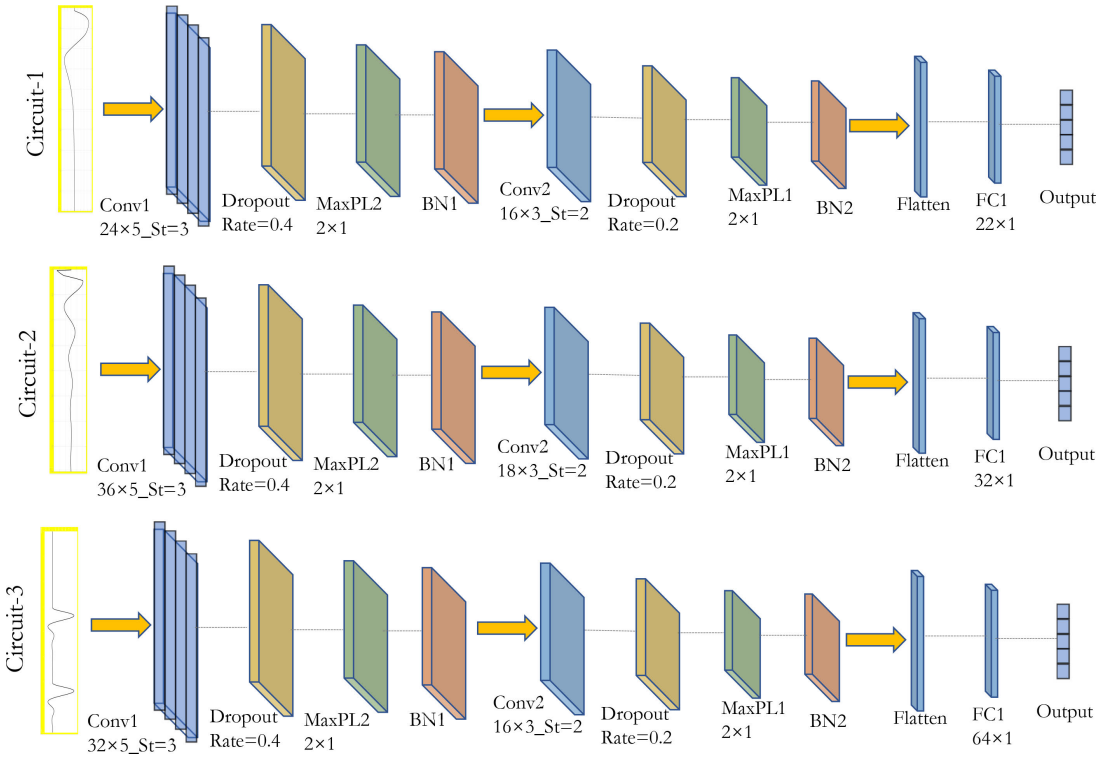


**FIGURE 2.** The detailed configuration of 1D-CNN model for three experimental circuits.

### B. DETAILED CONFIGURATION FOR THREE CIRCUITS

As aforementioned in section 2.1, the core component of the proposed 1D-CNN architecture is *Conv* block, which consists of four main layers, including the Conv layer, dropout layer, PL layer and the BN layer. Prior to implementing the signals to the CNN classifier, response signals of the analog circuit that are sampled as sequential time series, will be preprocessed by the normalization. Figure 2 illustrates the configuration of 1D-CNN model for three circuits. It should be indicated that ReLU is selected as the activation function. Moreover, the max-pooling function is used for the PL layer, while the batch size varies from 20 to 60.

As shown in Figure 2, low-level layers have larger number of kernels and high-level layers have smaller numbers of kernels. For example, in the test circuit-1, the number of kernels in Conv-1 is 24, while receptive field of each kernel is 5. On the other hand, the number of kernels in Conv-2 is 16, while receptive field of each kernel is 3. Therefore, the kernel depth in Con-2 is 24 as the depth is the number of channels that is decided by feature maps of the previous layer. In each *Conv* layer, the input sequence is separated into several vectors in accordance with the number of kernels of this *Conv* layer so that Conv-1 is 24 and Conv-2 is 16. This pyramid architecture can reduce the number of learnable parameters. Through these *Conv* blocks, a hierarchy of low- to high-level features originating from the input 1D-sequence can be learned, while the redundancy or unnecessary features reduce.

## III. SIMULATION EXPERIMENTS

In this section, three cases are studied in analog circuit fault diagnosis to evaluate the performance of the proposed method. Sallen-Key band pass filter and four-opamp biquad high-pass filer are the most representative subjects to investigate the analog circuits fault diagnosis. Meanwhile, these filters can be simply applied to verify the performance of the proposed method. On the other hand, the leapfrog filter is a more complex filter circuit with more critical components, which is widely applied for the fault diagnosis [22]. Therefore, the leapfrog filter is employed in the present study to demonstrate the wide applicability of the proposed 1D-CNN model. Circuit modeling and signal processing are performed in the MATLAB/Simulink platform, where the data collection of fault patterns and 1D-CNN training can be integrated seamlessly. Generally, the analog circuit fault diagnosis is mainly divided into two cases with respect to the fault type. These cases are single faults and multiple faults [43].

*Single faults*: In case of the single fault, one of the critical components fails, while no other component is in the failure state. In this case, faulty impulse responses can be processed with the feature extraction to implement the real-time diagnosis. Generally, single faults have the highest probability of fault occurrence in the system [4].

*Multiple faults or coupling faults*: In this case, two or multiple components fail simultaneously or the faulty component causes the failure of other associated components. Since the coupling fault in this case is mostly caused by

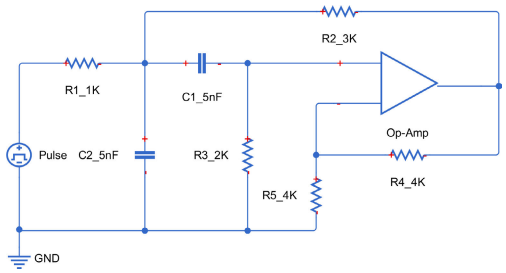


**FIGURE 3.** Salley-Key Bandpass Filter model.

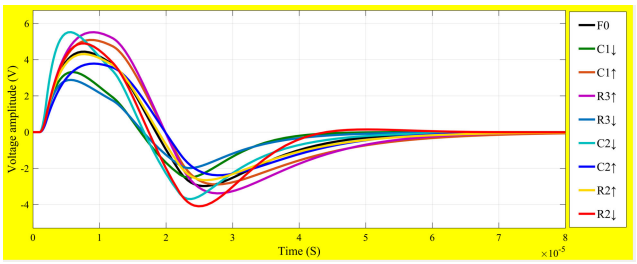


**FIGURE 4.** Raw output signals of different fault patterns in circuit-1.

switching circuits, performing an efficient diagnosis is a great challenge. It should be indicated that multiple faults have the same processing methods with the single faults. Studies show that multiple faults have lower probability of occurrence in comparison with the single fault case.

Therefore, the proposed 1D-CNN method is validated through single fault simulation in the analog circuit modeling. First, features of single fault patterns in the example circuits modeling are extracted and results are visualized in section 3.1. Second, the fault classification experiment is conducted to verify the performance of the fault diagnosis in section 3.2.

### *A. FEATURE EXTRACTION AND VISUALIZATION*

#### 1) EXAMPLE CIRCUIT 1

In this experiment, Sallen-Key bandpass filter circuit is modeled and soft faults are simulated to occur in four critical components. Figure 3 illustrates the configuration of such filter. The tolerance values of resistors and capacitors are set to 5% and 10%, respectively. Considering the rationality of faults setting, normal values of the components R2, R3, C1 and C2 have more impact on the center frequency. Accordingly, these four critical components are determined as fault injection devices through the sensitivity analysis. Fault free condition and different soft faults are simulated in R2, R3, C1 and C2 with 50% lower and higher variation than their nominal values. The single pulse of 5V pick amplitude with duration of 80$\mu$s is applied as the input signal. Figure 4 presents the response signals with different fault patterns, where $\downarrow$ and $\uparrow$ symbols donate higher and lower variations than the nominal variation, respectively. F0 is the fault free condition. Moreover, to further evaluate the performance of the proposed 1D-CNN method, 5% (of the voltage range) white Gaussian noise and 3% (of the sampling time) shift variance are added to the raw response signals.

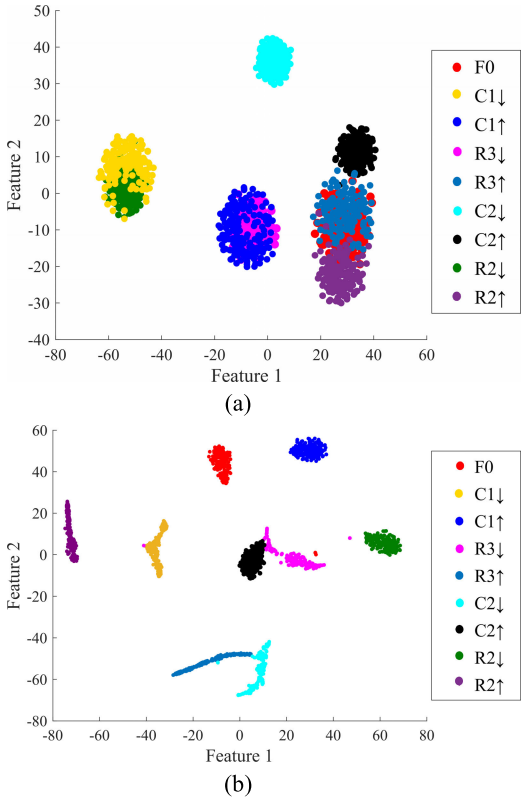


**FIGURE 5.** Feature visualization of the 1D-CNN FC layer in the circuit-1 (a) input data (b) output data of hidden FC layer.

Then the dataset of each fault with almost the same fault signature (hereafter called the ambiguity set) should be produced in the fault dictionary. Accordingly, the Monte-Carlo analysis is performed to obtain a large number of instances for a fault mode that are used for learning and evaluating the neural network parameters. Time series signal for each fault type is treated as one input instance to perform the analysis. Then the Monte-Carlo analysis is conducted 300 times and 300 groups of fault instances are collected as the ''ambiguity sets''. Each incipient fault class is equally divided into training and testing dataset with 150 samples. The training dataset is applied for constructing the 1D-CNN modeling with feature extraction and fault classification, and the testing data is used for validation study.

As shown in Figure 2, the configuration of 1D-CNN model for circuit-1 is constructed with 2 *Conv* blocks, a FC layer and a softmax classifier. The response signal of each fault type in this circuit is sampled with dimension of $400\times1$ and output of FC layer is $22\times1$. The convolutional kernel sizes of *Conv*-1 and *Conv*-2 blocks are 5 and 3, respectively. The measured signals are first normalized and then used as the input data of 1D-CNN. For illustrating results of the feature extraction more clearly, the t-SNE technique is employed to provide a two-dimension representation feature of the input data and output of 1D-CNN FC layer. Obtained results are presented in Figure 5.

Feature extraction results of circuit-1 indicate that the deep and intrinsic feature of each incipient faults can be separated

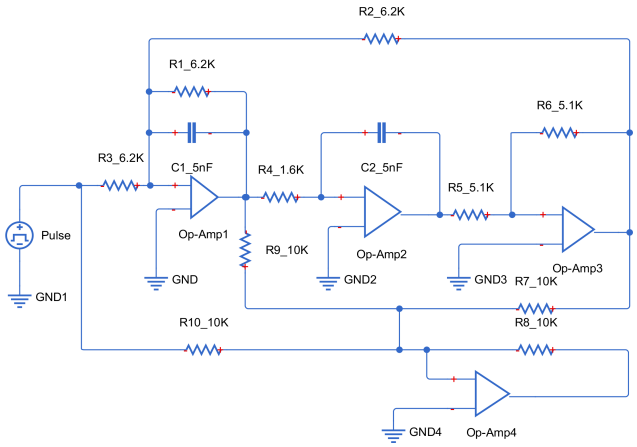


**FIGURE 6.** Four-opamp biquad high-pass filter model.

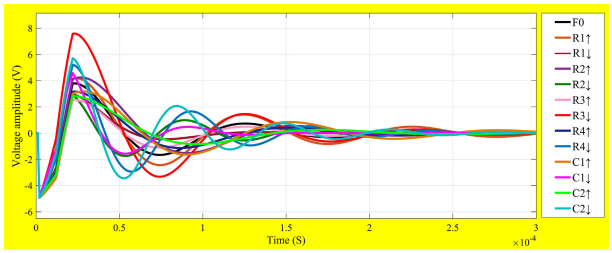


**FIGURE 7.** Raw output signals of different fault patterns in circuit-2.

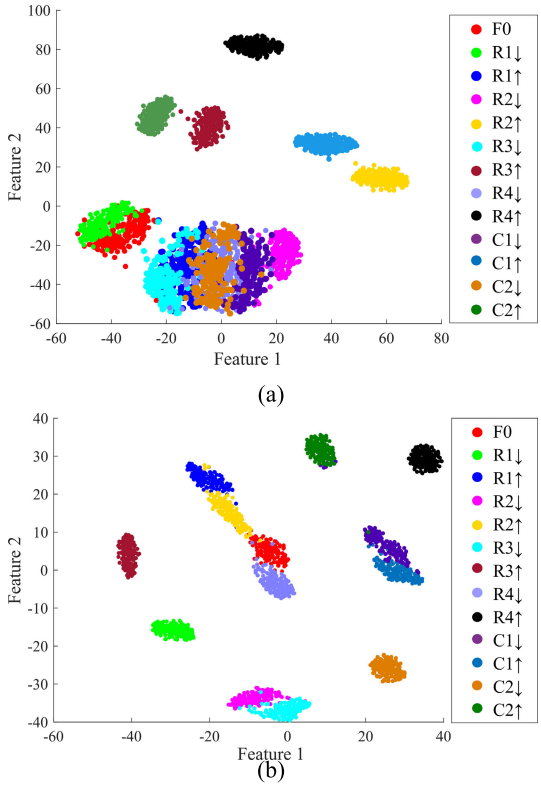


**FIGURE 8.** Feature visualization of the 1D-CNN FC layer in circuit-2 (a) input data (b) output data of hidden FC layer.

from raw signals by the proposed 1D-CNN model. Figure 5 shows that signals in the fault free condition represented by red dots has two outliers, which is close to region R3↓. Similarly, signals in R3↓ condition have two outliers, which approach to C1↓ and R2↑ regions. Meanwhile, there are slight overlapping between the R3↓ and C2↑ regions, C2↓ and R3↑ regions. However, after implementing kernel filters and sub-sampling layers, the FC layer can extract abstract and higher-level features of soft fault patterns, which has obtained great performance compared with raw data. The feature extractor of *Conv* blocks and FC layer provide basis for successive fault diagnosis in analog circuits.

### 2) EXAMPLE CIRCUIT 2

Four-opamp biquad high-pass filter is considered in the second test circuit. The circuit model and nominal values of all components are shown in Figure6. The tolerance values of resistors and capacitors have same setting with those of the Salley-Key bandpass filter in the foregoing section. Regarding the rationality of faults setting, components R1, R2, R3, R4, C1 and C2 are selected as the experimental devices with 50% lower and higher variation than their nominal values through the sensitivity analysis. Input signal is a single pulse of 5V pick amplitude with 10$\mu$s duration in the time domain, and raw output response signals of all incipient faults and fault free condition are shown in Figure 7. The simulation is conducted with 300$\mu$s duration and output time series of 12 fault modes are obtained. Then the noise is added to the raw signals as same as circuit-1.

Then the Monte-Carlo simulation is performed to produce 300 samples of each fault mode, which are equally separated into the training and the testing datasets. Similarly, the 1D-CNN model for this circuit is constructed with 2 blocks, a FC layer and a softmax classifier. The response signal of each incipient fault in this circuit is sampled with dimension of 600×1 and output of FC layer is 32×1. The number of kernels in Conv-1 and Conv-2 is 36 and 18, while receptive field of each kernel is 5 and 3, respectively. The max pooling kernels with length 2 are designed in all *Conv* blocks. Then the t-SNE technique is applied to visualize the input data and output data of to demonstrate the feature extraction results.

Figure 8 indicates that the 1D-CNN model can separate different fault patterns apparently. Intuitively, it shows that some fault patterns have slight overlapping between R3↓ and R2↓ regions, C1↓ and C2↑ regions, R1↓ and R2↑ regions, R4↓ and fault free regions. In addition, C2↑ and C1↓ has a few outliers in each other's regions. However, comparing with the results of raw data, the regions of each fault type have clear boundary after processing by 1D-CNN, which demonstrates its good performance in feature extraction further.

### 3) EXAMPLE CIRCUIT 3

In this section, a more complex analog circuit model is presented to illustrate the feature extraction performance of the 1D-CNN. A leapfrog filter circuit model with normal values of all components is presented in Figure 9.

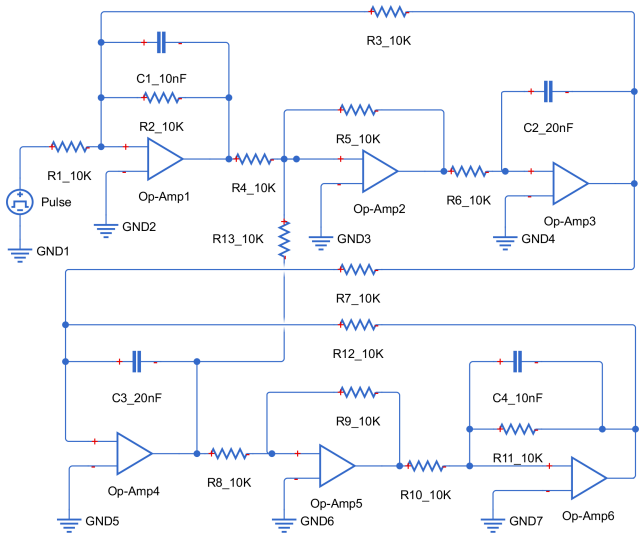


**FIGURE 9.** Leapfrog filter circuit.

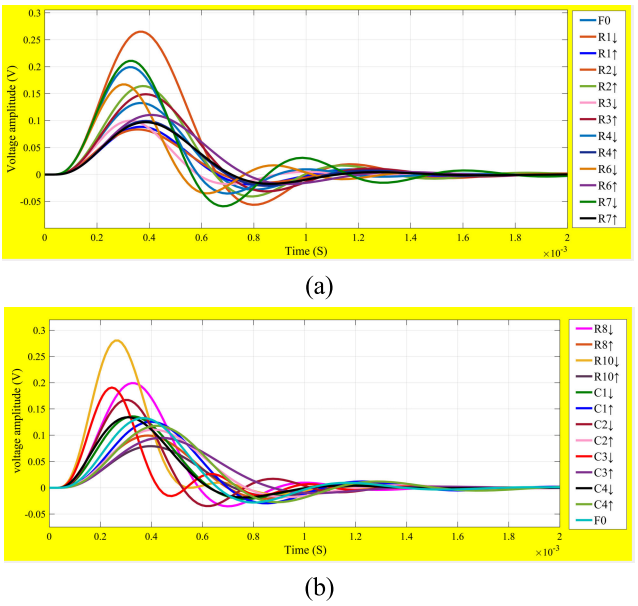


**FIGURE 10.** Raw output signals of different fault patterns in circuit-3 (a) soft faults in R1, R2, R3, R4, R6, and R7 (b) soft faults in R8, R10, C1, C2, C3, and C4.

It should be indicated that most components in this circuit are sensitive to the parameters of the response waveform, including the center frequency, voltage maximum and the bandwidth. In this regard, the components R1, R2, R3, R4, R6, R7, R8, R9, R10, C1, C2, C3, and C4 which have remarkable impact on the waveform parameters should be simulated in the failure state with 50% lower and higher variation than their nominal values. The rationality of fault occurrence is fully considered by the fault setting to reflect the inherent characteristics of each faulty component. Input signal is a single pulse of 5V pick amplitude with 200$\mu$s duration in the time domain. The white noise is added to the simulated signals as above two circuits. In order to show the raw response signals more clearly, the waveforms of signals

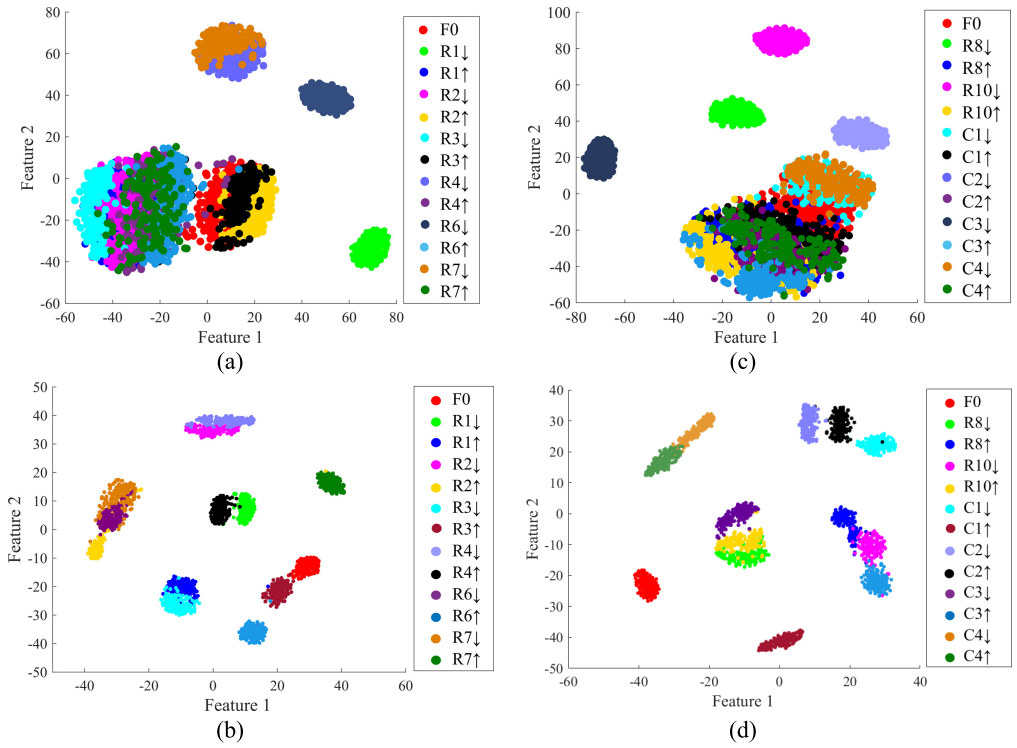


**FIGURE 11.** Feature visualization of 1D-CNN FC layer in circuit-3 (a) soft faults in R1, R2, R3, R4, R6, and R7 (b) soft faults in R8, R10, C1, C2, C3, and C4.

**TABLE 1. Comparing the classification accuracy of different methods in Circuit-1.**

| Fault Class | Classification accuracy (%) | | | |
|---|---|---|---|---|
| | 1D-CNN | ANFIS | DBN | WNN |
| F0 | 98.1 | 98.7 | **100** | **100** |
| C1↓ | 94.4 | 94.2 | **97.4** | 95.2 |
| C1↑ | **100** | 94.6 | 95.7 | 91.5 |
| C2↓ | 97.6 | **100** | 98.7 | 94.2 |
| C2↑ | **100** | 98.1 | 94.6 | 95.0 |
| R2↓ | **100** | 99.6 | 95.3 | 93.5 |
| R2↑ | 94.7 | 96.5 | **100** | 99.2 |
| R3↓ | **98.8** | 93.4 | 97.2 | 94.3 |
| R3↑ | 95.6 | **97.5** | 96.7 | 87.5 |

**TABLE 2. Comparing the classification accuracy of different methods in Circuit-2.**

| Fault Class | Classification accuracy (%) | | | |
|---|---|---|---|---|
| | 1D-CNN | ANFIS | DBN | WNN |
| F0 | 96.3 | 98.4 | **100** | 97.6 |
| R1↑ | 97.2 | **100** | 95.7 | 96.2 |
| R1↓ | **100** | 98.3 | 96.2 | 94.2 |
| R2↑ | 93.5 | 94.9 | 94.8 | **96.8** |
| R2↓ | 96.3 | 95.2 | **100** | 97.1 |
| R3↑ | **100** | 96.1 | 95.0 | 92.7 |
| R3↓ | 94.5 | **100** | 93.6 | 93.6 |
| R4↑ | **100** | 91.5 | 93.1 | 91.3 |
| R4↓ | **94.6** | 90.8 | 92.5 | 88.7 |
| C1↑ | 93.7 | 94.8 | **96.3** | 94.0 |
| C1↓ | **98.3** | 97.4 | 96.3 | 97.2 |
| C2↑ | **97.6** | 93.9 | 90.4 | 91.9 |
| C2↓ | **100** | 92.5 | 91.5 | 87.7 |

are separated. Figures 10 (a) and 10 (b) illustrate the obtained results.

The response signal of each fault in this circuit is sampled with dimension of 800×1 and output of FC layer is 64×1. As shown in Figure 2, the number of kernels in Conv-1 ad Conv-2 is 32 and 16, while receptive field of each kernel is 5 and 3, respectively. After feature extraction, the feature visualization results of raw data and output data are presented in Figure 11 using t-SNE technique.

Experimental results prove that the 1D-CNN model has reasonable performance in extracting deep features for soft faults in analog circuits. Meanwhile, it can implement the filtering of interference noise in the feature extraction process. Comparing the visualization results presented in Figures 11(a) and 11(b), 11(c) and 11(d), it is concluded that learned features by the 1D-CNN achieves a better separability. A large area of overlapping if found in raw data visualization results, but a slighter overlapping exists in the output data of the FC layer. Mapped features of the 1D-CNN can be clustered well for all fault types, indicating the good

**TABLE 3. Comparing the classification accuracy of different methods in Circuit-3.**

| Fault Class | Classification accuracy (%) | | | |
|---|---|---|---|---|
| | 1D-CNN | ANFIS | DBN | WNN |
| F0 | **99.2** | 95.7 | 97.8 | 94.6 |
| R1↓ | **97.7** | 91.5 | 93.4 | 95.7 |
| R1↑ | 90.5 | 92.3 | **93.6** | 88.3 |
| R2↓ | 94.8 | 91.5 | 95.0 | 93.2 |
| R2↑ | 92.7 | **98.4** | 91.4 | 90.5 |
| R3↓ | **96.8** | 92.9 | 92.5 | 90.3 |
| R3↑ | 98.4 | 93.8 | **100** | 96.8 |
| R4↓ | 90.7 | 94.4 | **95.4** | 93.4 |
| R4↑ | **93.1** | 89.2 | 91.1 | 89.5 |
| R6↓ | 90.2 | **94.6** | 92.7 | 93.0 |
| R6↑ | **100** | 98.3 | 100 | 93.6 |
| R7↓ | **92.7** | 92.3 | 91.4 | 90.6 |
| R7↑ | **97.4** | 91.6 | 92.4 | 91.4 |
| R8↓ | **97.3** | 95.3 | 93.7 | 94.6 |
| R8↑ | 95.4 | 94.3 | **96.5** | 88.3 |
| R10↓ | 93.0 | 91.0 | **94.1** | 93.4 |
| R10↑ | 94.6 | 98.4 | 98.4 | **100** |
| C1↓ | 92.5 | 91.7 | **95.3** | 92.4 |
| C1↑ | **100** | 97.3 | 97.5 | 100 |
| C2↓ | **98.8** | 88.5 | 93.5 | 94.2 |
| C2↑ | **94.3** | 92.5 | 93.7 | 89.6 |
| C3↓ | 97.9 | 93.8 | **99.1** | 90.3 |
| C3↑ | 97.5 | 95.6 | **98.0** | 91.4 |
| C4↓ | **96.5** | 89.3 | 92.8 | 95.3 |
| C4↑ | **97.4** | 91.5 | 93.9 | 90.5 |

performance of feature representation ability of the proposed model. Meanwhile, the feature extraction results are in good consistency with fault classification results shown in Table 4.

### B. CLASSIFICATION EXPERIMENT TO PERFORM FAULT DIAGNOSIS

Feature extraction and selection is an important stage for fault classification aiming to find an effective fault diagnosis method. Experimental circuits include the Salley-Key bandpass filter (Circuit-1), Four-opamp biquad high-pass filter (Circuit-2), and the leapfrog filter (Circuit-3). The circuit model and parameter settings, including the noise added to the dataset of circuit-3, are the same with those of section 3.1. In order to evaluate the performance of the proposed method, results obtained from the 1D-CNN classifier are compared with those of other classification methods, including ANFIS [22], DBN [17] and UFK-WNN [20]. All of these methods are based on the neural network algorithm. For each incipient fault pattern, 300 groups labeled 1-D time series are divided equally into 150 groups of training data and 150 groups of testing samples. It should be indicated the common 1D-CNN model with the same configuration as

**TABLE 4.** Confusion matrix of the testing results based on 1D-CNN in Circuit-1, Circuit-2 and Circuit-3.

| Actual class \ Predicted class | F0 | C1↓ | C1↑ | C2↓ | C2↑ | R2↓ | R2↑ | R3↓ | R3↑ |
|---|---|---|---|---|---|---|---|---|---|
| F0 | 147 | 0 | 0 | 0 | 0 | 0 | 0 | 0 | 3 |
| C1↓ | 0 | 143 | 2 | 0 | 0 | 0 | 0 | 5 | 0 |
| C1↑ | 0 | 0 | 150 | 0 | 0 | 0 | 0 | 0 | 0 |
| C2↓ | 0 | 0 | 0 | 147 | 0 | 0 | 0 | 3 | 0 |
| C2↑ | 0 | 0 | 0 | 0 | 150 | 0 | 0 | 0 | 0 |
| R2↓ | 0 | 0 | 0 | 0 | 0 | 150 | 0 | 0 | 0 |
| R2↑ | 0 | 0 | 2 | 0 | 0 | 4 | 144 | 0 | 0 |
| R3↓ | 0 | 0 | 0 | 0 | 0 | 2 | 0 | 148 | 0 |
| R3↑ | 4 | 0 | 0 | 0 | 0 | 0 | 0 | 0 | 146 |

| Actual class \ Predicted class | F0 | R1↑ | R1↓ | R2↑ | R2↓ | R3↑ | R3↓ | R4↑ | R4↓ | C1↑ | C1↓ | C2↑ | C2↓ |
|---|---|---|---|---|---|---|---|---|---|---|---|---|---|
| F0 | 145 | 0 | 0 | 3 | 0 | 0 | 0 | 0 | 2 | 0 | 0 | 0 | 0 |
| R1↑ | 0 | 144 | 0 | 4 | 0 | 0 | 0 | 0 | 0 | 0 | 0 | 0 | 2 |
| R1↓ | 0 | 0 | 150 | 0 | 0 | 0 | 0 | 0 | 0 | 0 | 0 | 0 | 0 |
| R2↑ | 6 | 5 | 0 | 139 | 0 | 0 | 0 | 0 | 0 | 0 | 0 | 0 | 0 |
| R2↓ | 0 | 0 | 0 | 0 | 144 | 0 | 6 | 0 | 0 | 0 | 0 | 0 | 0 |
| R3↑ | 0 | 0 | 0 | 0 | 0 | 150 | 0 | 0 | 0 | 0 | 0 | 0 | 0 |
| R3↓ | 0 | 0 | 0 | 0 | 5 | 0 | 145 | 0 | 0 | 0 | 0 | 0 | 0 |
| R4↑ | 0 | 0 | 0 | 0 | 0 | 0 | 0 | 150 | 0 | 0 | 0 | 0 | 0 |
| R4↓ | 4 | 0 | 0 | 0 | 0 | 0 | 0 | 0 | 146 | 0 | 0 | 0 | 0 |
| C1↑ | 0 | 0 | 0 | 0 | 0 | 0 | 0 | 0 | 0 | 143 | 7 | 0 | 0 |
| C1↓ | 0 | 0 | 0 | 0 | 0 | 0 | 0 | 0 | 0 | 6 | 144 | 0 | 0 |
| C2↑ | 0 | 0 | 0 | 0 | 0 | 0 | 0 | 0 | 0 | 0 | 1 | 149 | 0 |
| C2↓ | 0 | 0 | 0 | 0 | 0 | 0 | 0 | 0 | 0 | 0 | 0 | 0 | 150 |

| Actual classes \ Predicted classes | F0 | R1↓ | R1↑ | R2↓ | R2↑ | R3↓ | R3↑ | R4↓ | R4↑ | R6↓ | R6↑ | R7↓ | R7↑ | R8↓ | R8↑ | R10↓ | R10↑ | C1↓ | C1↑ | C2↓ | C2↑ | C3↓ | C3↑ | C4↓ | C4↑ |
|---|---|---|---|---|---|---|---|---|---|---|---|---|---|---|---|---|---|---|---|---|---|---|---|---|---|
| F0 | 148 | 0 | 0 | 0 | 0 | 0 | 2 | 0 | 0 | 0 | 0 | 0 | 0 | 0 | 0 | 0 | 0 | 0 | 0 | 0 | 0 | 0 | 0 | 0 | 0 |
| R1↓ | 0 | 146 | 0 | 0 | 0 | 0 | 0 | 0 | 4 | 0 | 0 | 0 | 0 | 0 | 0 | 0 | 0 | 0 | 0 | 0 | 0 | 0 | 0 | 0 | 0 |
| R1↑ | 0 | 0 | 136 | 0 | 0 | 10 | 0 | 0 | 0 | 0 | 0 | 0 | 0 | 0 | 0 | 0 | 0 | 0 | 0 | 0 | 4 | 0 | 0 | 0 | 0 |
| R2↓ | 0 | 0 | 0 | 139 | 0 | 0 | 0 | 8 | 0 | 0 | 0 | 0 | 0 | 0 | 0 | 0 | 0 | 0 | 0 | 0 | 0 | 0 | 0 | 3 | 0 |
| R2↑ | 0 | 0 | 0 | 0 | 141 | 0 | 6 | 0 | 0 | 0 | 0 | 2 | 1 | 0 | 0 | 0 | 0 | 0 | 0 | 0 | 0 | 0 | 0 | 0 | 0 |
| R3↓ | 0 | 8 | 0 | 0 | 0 | 140 | 0 | 0 | 0 | 0 | 0 | 0 | 0 | 0 | 0 | 0 | 0 | 2 | 0 | 0 | 0 | 0 | 0 | 0 | 0 |
| R3↑ | 2 | 0 | 0 | 0 | 0 | 0 | 148 | 0 | 0 | 0 | 0 | 0 | 0 | 0 | 0 | 0 | 0 | 0 | 0 | 0 | 0 | 0 | 0 | 0 | 0 |
| R4↓ | 0 | 0 | 0 | 11 | 0 | 0 | 0 | 136 | 0 | 0 | 0 | 0 | 0 | 0 | 0 | 0 | 0 | 0 | 0 | 0 | 0 | 3 | 0 | 0 | 0 |
| R4↑ | 0 | 1 | 0 | 0 | 0 | 0 | 0 | 0 | 141 | 0 | 0 | 0 | 0 | 0 | 0 | 0 | 0 | 0 | 0 | 3 | 0 | 0 | 0 | 0 | 5 |
| R6↓ | 0 | 0 | 0 | 0 | 7 | 0 | 0 | 0 | 0 | 135 | 0 | 8 | 0 | 0 | 0 | 0 | 0 | 0 | 0 | 0 | 0 | 0 | 0 | 0 | 0 |
| R6↑ | 0 | 0 | 0 | 0 | 0 | 0 | 0 | 0 | 0 | 0 | 150 | 0 | 0 | 0 | 0 | 0 | 0 | 0 | 0 | 0 | 0 | 0 | 0 | 0 | 0 |
| R7↓ | 0 | 0 | 0 | 0 | 1 | 0 | 4 | 0 | 0 | 0 | 0 | 145 | 0 | 0 | 0 | 0 | 0 | 0 | 0 | 0 | 0 | 0 | 0 | 0 | 0 |
| R7↑ | 0 | 0 | 0 | 0 | 0 | 0 | 0 | 0 | 0 | 0 | 0 | 0 | 150 | 0 | 0 | 0 | 0 | 0 | 0 | 0 | 0 | 0 | 0 | 0 | 0 |
| R8↓ | 0 | 0 | 0 | 0 | 0 | 0 | 0 | 0 | 0 | 0 | 0 | 0 | 0 | 146 | 0 | 0 | 4 | 0 | 0 | 0 | 0 | 0 | 0 | 0 | 0 |
| R8↑ | 0 | 0 | 0 | 0 | 0 | 0 | 0 | 0 | 0 | 0 | 0 | 0 | 0 | 0 | 142 | 7 | 0 | 0 | 0 | 0 | 0 | 0 | 1 | 0 | 0 |
| R10↓ | 0 | 0 | 0 | 0 | 0 | 0 | 0 | 0 | 0 | 0 | 0 | 0 | 0 | 0 | 8 | 140 | 0 | 0 | 0 | 0 | 0 | 0 | 2 | 0 | 0 |
| R10↑ | 0 | 0 | 0 | 0 | 0 | 0 | 0 | 0 | 0 | 0 | 0 | 0 | 0 | 6 | 0 | 0 | 143 | 0 | 0 | 0 | 0 | 1 | 0 | 0 | 0 |
| C1↓ | 0 | 0 | 0 | 0 | 0 | 0 | 8 | 0 | 0 | 0 | 0 | 0 | 0 | 0 | 0 | 0 | 0 | 140 | 0 | 0 | 2 | 0 | 0 | 0 | 0 |
| C1↑ | 0 | 0 | 0 | 0 | 0 | 0 | 0 | 0 | 0 | 0 | 0 | 0 | 0 | 0 | 0 | 0 | 0 | 0 | 150 | 0 | 0 | 0 | 0 | 0 | 0 |
| C2↓ | 0 | 0 | 0 | 0 | 0 | 0 | 0 | 0 | 2 | 0 | 0 | 0 | 0 | 0 | 0 | 0 | 0 | 0 | 0 | 148 | 0 | 0 | 0 | 0 | 0 |
| C2↑ | 0 | 0 | 5 | 0 | 0 | 0 | 0 | 0 | 0 | 0 | 0 | 0 | 0 | 0 | 0 | 0 | 0 | 3 | 0 | 0 | 142 | 0 | 0 | 0 | 0 |
| C3↓ | 0 | 0 | 0 | 0 | 0 | 0 | 0 | 3 | 0 | 0 | 0 | 0 | 0 | 0 | 0 | 0 | 0 | 2 | 0 | 0 | 0 | 145 | 0 | 0 | 0 |
| C3↑ | 0 | 0 | 0 | 0 | 0 | 0 | 0 | 0 | 0 | 0 | 0 | 0 | 0 | 0 | 0 | 4 | 0 | 0 | 0 | 0 | 0 | 0 | 146 | 0 | 0 |
| C4↓ | 0 | 0 | 0 | 0 | 0 | 0 | 0 | 0 | 0 | 0 | 0 | 0 | 0 | 0 | 0 | 0 | 0 | 0 | 0 | 0 | 0 | 0 | 0 | 145 | 5 |
| C4↑ | 0 | 0 | 0 | 0 | 0 | 0 | 0 | 0 | 3 | 0 | 0 | 0 | 0 | 0 | 0 | 0 | 0 | 0 | 0 | 0 | 0 | 0 | 0 | 4 | 143 |

the model in feature extraction experiments is used for the feature extraction and fault classification for one circuit, but the output data is from the FC layer in the feature extraction and classification results is from softmax layer. The 10-fold cross-validation experimental results of fault classification are provided in Tables 1, 2, and 3.In order to present the actual and predicted categories of each fault type intuitively, the confusion matrix (i.e. the error matrix in the supervised learning) of testing results are obtained through the 1D-CNN in one experiment. Table 4 presents the obtained results accordingly.

Comparing the classification results obtained from different methods indicate that the fault diagnosis performance of the 1D-CNN method has high accuracy even when input signals are polluted by the noise. With the powerful filter capability, the 1D-CNN method shows superior performance to ANFIS, DBN and WNN methods in accuracy and anti-interference of classification. It is found that the classification accuracy of 1D-CNN, ANFIS, DBN and WNN methods reach 97.7%, 97.0%, 97.3% and 94.5%, respectively for circuit-1, and 97.1%, 95.7%, 95.0% and 93.8%, respectively for circuit-2. Furthermore, results have some differences for various faults modes. For example, C1↑ and C1↓, R4↑ and R4↓ have lower diagnosis accuracy, which originates from their similar response signals in circuit-2. Moreover, the average classification accuracy of ANFIS, DBN, and UKF-WNN methods for circuit-3 reaches 93.4%, 94.9% and 92.8%, while that of the proposed 1D-CNN method reaches 95.6%, which demonstrates the reasonable performance of the proposed method in the fault diagnosing. Based on the confusion matrix of testing results obtained from the 1D-CNN method in one experiment, it is concluded that most fault types can be classified into accurate categories with a small number of true negatives. Furthermore, comparing the two results of feature extraction and confusion matrix, shows that they are consistent with each other, where the distinct feature extraction result promotes the classification accuracy. It can be concluded that the 1D-CNN method can achieve satisfactory results with anti-interference and stable characteristics in soft fault diagnosing of analog circuits.

## IV. CONCLUSION

This paper proposes an analog circuit fault diagnosis method using the a compact 1D-CNN model. The proposed intelligent diagnosis model employs a supervised machine learning approach for fault classification with feature extraction and visualization. The adaptive mechanism is implemented by constructing *Conv* blocks so that hierarchical features can be obtained through these blocks. Compared with existing NN methods, the proposed 1D-CNN model can be simply designed for more complex analog circuits and can distinguish various signals of fault patterns. The convolution kernels (filters) are utilized in the training model with capability of learning local and hierarchical representations from raw signals. These kernels not only improve the classification accuracy, but also guarantee the anti-interference performance of fault diagnosis method, which makes it more suitable for real-time fault detection and monitoring. Then the performance of the proposed method is evaluated through three analog circuit examples. However, the main drawback of the proposed method is that training the 1D-CNN model requires more accurate and larger labeled datasets. In the near future, it is intended to focus on the more data-driven fault diagnostic techniques with data argumentation methods through the unsupervised way.

## REFERENCES

[1] M. Aminian and F. Aminian, "Neural-network based analog-circuit fault diagnosis using wavelet transform as preprocessor," *IEEE Trans. Circuits Syst. II, Analog Digit. Signal Process.*, vol. 47, no. 2, pp. 151–156, Feb. 2000.
[2] M. Hu, H. Wang, G. Hu, and S. Yang, "Soft fault diagnosis for analog circuits based on slope fault feature and BP neural networks," *Tinshhua Sci. Technol.*, vol. 12, no. S1, pp. 26–31, Jul. 2007.
[3] S. Tang, Z. Li, and L. Chen, "Fault detection in analog and mixed-signal circuits by using Hilbert–Huang transform and coherence analysis," *Microelectron. J.*, vol. 46, no. 10, pp. 893–899, Oct. 2015.
[4] C. Zhang, Y. He, L. Yuan, and S. Xiang, "Analog circuit incipient fault diagnosis method using DBN based features extraction," *IEEE Access*, vol. 6, pp. 23053–23064, 2018.
[5] M. Pecht and R. Jaai, "A prognostics and health management roadmap for information and electronics-rich systems," *Microelectron. Rel.*, vol. 50, no. 3, pp. 317–323, Mar. 2010.
[6] Z. Liu, T. Liu, J. Han, S. Bu, X. Tang, and M. Pecht, "Signal model-based fault coding for diagnostics and prognostics of analog electronic circuits," *IEEE Trans. Ind. Electron.*, vol. 64, no. 1, pp. 605–614, Jan. 2017.
[7] C. Xiaomei, M. Xiaofeng, and W. Guohua, "A modified simulation-based multi-signal modeling for electronic system," *J. Electron. Test.*, vol. 28, no. 2, pp. 155–165, Apr. 2012.
[8] T. Zhang and T. Li, "Analog circuit soft fault diagnosis utilizing matrix perturbation analysis," *Analog Integr. Circuit Signal Process.*, vol. 100, no. 1, pp. 181–192, Jul. 2019.
[9] A. Kumar and A. Singh, "Fuzzy classifier for fault diagnosis in analog electronic circuits," *ISA Trans.*, vol. 52, no. 6, pp. 816–824, Nov. 2013.
[10] T. Sun, D. Zhou, Y. Zhu, and M. V. Basin, "Stability, $l_2$-gain analysis, and parity space-based fault detection for discrete-time switched systems under dwell-time switching," *IEEE Trans. Syst., Man, Cybern., Syst.*, to be published, doi: 10.1109/tsmc.2018.2866876.
[11] Y. Deng and G. Chai, "Soft fault feature extraction in nonlinear analog circuit fault diagnosis," *Circuits Syst. Signal Process.*, vol. 35, no. 12, pp. 4220–4248, Dec. 2016.
[12] C. Yang, L. Zhen, and C. Hu, "Fault diagnosis of analog filter circuit based on genetic algorithm," *IEEE Access*, vol. 7, pp. 54969–54980, 2019.
[13] Y. Cui, J. Shi, and Z. Wang, "Analog circuit test point selection incorporating discretization-based fuzzification and extended fault dictionary to handle component tolerances," *J. Electron. Test.*, vol. 32, no. 6, pp. 661–679, Dec. 2016.
[14] D. Liu and J. A. Starzyk, "A generalized fault diagnosis method in dynamic analogue circuits," *Int. J. Circuits Theory Appl.*, vol. 30, no. 5, pp. 487–510, Sep. 2002.
[15] M. Tadeusiewicz, S. Halgas, and M. Korzybski, "An algorithm for soft-fault diagnosis of linear and nonlinear circuits," *IEEE Trans. Circuits Syst. I. Fundam. Theory Appl.*, vol. 49, no. 11, pp. 1648–1653, Nov. 2002.
[16] C. Yang, J. Yang, Z. Liu, and S. Tian, "Complex field fault modeling-based optimal frequency selection in linear analog circuit fault diagnosis," *IEEE Trans. Instrum. Meas.*, vol. 63, no. 4, pp. 813–825, Apr. 2014.
[17] G. Zhao, X. Liu, B. Zhang, Y. Liu, G. Niu, and C. Hu, "A novel approach for analog circuit fault diagnosis based on deep belief network," *Measurement*, vol. 121, pp. 170–178, Jun. 2018.
[18] Y. Xiao and Y. He, "A novel approach for analog fault diagnosis based on neural networks and improved kernel PCA," *Neurocomputing*, vol. 74, no. 7, pp. 1102–1115, Mar. 2011.
[19] Y. Xiao and L. Feng, "A novel neural-network approach of analog fault diagnosis based on kernel discriminant analysis and particle swarm optimization," *Appl. Soft Comput.*, vol. 12, no. 2, pp. 904–920, Feb. 2012.
[20] G. Xu-sheng, G. Wen-ming, D. Zhe, and L. Wei-dong, "Research on WNN soft fault diagnosis for analog circuit based on adaptive UKF algorithm," *Appl. Soft Comput.*, vol. 50, pp. 252–259, Jan. 2017.

[21] D. Binu and B. S. Kariyappa, "RideNN: A new rider optimization algorithm-based neural network for fault diagnosis in analog circuits," *IEEE Trans. Instrum. Meas.*, vol. 68, no. 1, pp. 2–26, Jan. 2019.
[22] A. Arabi, N. Bourouba, A. Belaout, and M. Ayad, "An accurate classifier based on adaptive neuro-fuzzy and features selection techniques for fault classification in analog circuits," *Integration*, vol. 64, pp. 50–59, Jan. 2019.
[23] P. Chen, L. Yuan, Y. He, and S. Luo, "An improved SVM classifier based on double chains quantum genetic algorithm and its application in analogue circuit diagnosis," *Neurocomputing*, vol. 211, pp. 202–211, Oct. 2016.
[24] Q. Ma, Y. He, and F. Zhou, "A new decision tree approach of support vector machine for analog circuit fault diagnosis," *Analog Integr. Circuits Signal Process.*, vol. 88, no. 3, pp. 455–463, Sep. 2016.
[25] A. Zhang, C. Chen, and B. Jiang, "Analog circuit fault diagnosis based UCISVM," *Neurocomputing*, vol. 173, pp. 1752–1760, Jan. 2016.
[26] W. Yu, Y. Sui, and J. Wang, "The faults diagnostic analysis for analog circuit based on FA-TM-ELM," *J. Electron. Test.*, vol. 32, no. 4, pp. 459–465, Aug. 2016.
[27] G. Xu-Sheng, Q. Hong, M. Xiang-Wei, W. Chun-Lan, and Z. Jie, "Research on ELM soft fault diagnosis of analog circuit based on KSLPP feature extraction," *IEEE Access*, vol. 7, pp. 92517–92527, 2019.
[28] L. Yuan, Y. He, J. Huang, and Y. Sun, "A new neural-network-based fault diagnosis approach for analog circuits by using kurtosis and entropy as a preprocessor," *IEEE Trans. Instrum. Meas.*, vol. 59, no. 3, pp. 586–595, Mar. 2010.
[29] Y. Tan, Y. He, C. Cui, and G. Qiu, "A novel method for analog faultdiagnosis based on neural networks and genetic algorithms," *IEEE Trans. Instrum. Meas.*, vol. 57, no. 11, pp. 2631–2639, Nov. 2008.
[30] H. Luo and Y. W. Jiang Cui, "A SVDD approach of fuzzy classification for analog circuit fault diagnosis with FWT as preprocessor," *Expert Syst. Appl.*, vol. 38, no. 8, pp. 10554–10561, Aug. 2011.
[31] A. Zhang, Y. Wang, and Z. Zhang, "Performance evaluation of analog circuit using improved LSSVR subject to data information uncertainty," *Neurocomputing*, vol. 151, pp. 461–470, Mar. 2015.
[32] X. Yuan, Z. Liu, Z. Miao, Z. Zhao, F. Zhou, and Y. Song, "Fault diagnosis of analog circuits based on IH-PSO optimized support vector machine," *IEEE Access*, vol. 7, pp. 137945–137958, 2019.
[33] J. Han, D. Zhang, X. Hu, L. Guo, J. Ren, and F. Wu, "Background prior-based salient object detection via deep reconstruction residual," *IEEE Trans. Circuits Syst. Video Technol.*, vol. 25, no. 8, pp. 1309–1321, Aug. 2015.
[34] Y. Qian, M. Bi, T. Tan, and K. Yu, "Very deep convolutional neural networks for noise robust speech recognition," *IEEE/ACM Trans. Audio, Speech, Language Process.*, vol. 24, no. 12, pp. 2263–2276, Dec. 2016.
[35] Y. Chen, H. Jiang, C. Li, X. Jia, and P. Ghamisi, "Deep feature extraction and classification of hyperspectral images based on convolutional neural networks," *IEEE Trans. Geosci. Remote Sens.*, vol. 54, no. 10, pp. 6232–6251, Oct. 2016.
[36] G. Cheng, P. Zhou, and J. Han, "Learning rotation-invariant convolutional neural networks for object detection in VHR optical remote sensing images," *IEEE Trans. Geosci. Remote Sens.*, vol. 54, no. 12, pp. 7405–7415, Dec. 2016.
[37] J. Han, D. Zhang, G. Cheng, L. Guo, and J. Ren, "Object detection in optical remote sensing images based on weakly supervised learning and high-level feature learning," *IEEE Trans. Geosci. Remote Sens.*, vol. 53, no. 6, pp. 3325–3337, Jun. 2015.
[38] D. Lai, X. Zhang, K. Ma, Z. Chen, W. Chen, H. Zhang, H. Yuan, and L. Ding, "Automated detection of high frequency oscillations in intracranial EEG using the combination of short-time energy and convolutional neural networks," *IEEE Access*, vol. 7, pp. 82501–82511, 2019.
[39] S. Kiranyaz, T. Ince, and M. Gabbouj, "Real-time patient-specific ecg classification by 1-D convolutional neural networks," *IEEE Trans. Biomed. Eng.*, vol. 63, no. 3, pp. 664–675, Mar. 2016.
[40] L. Eren, T. Ince, and S. Kiranyaz, "A generic intelligent bearing fault diagnosis system using compact adaptive 1D CNN classifier," *J. Signal Process. Syst.*, vol. 91, no. 2, pp. 179–189, Feb. 2019.
[41] D. Peng, Z. Liu, H. Wang, Y. Qin, and L. Jia, "A novel deeper one-dimensional CNN with residual learning for fault diagnosis of wheelset bearings in high-speed trains," *IEEE Access*, vol. 7, pp. 10278–10293, 2019.
[42] L. Yu, Y. Zhang, H. Han, L. Zhang, and F. Wu, "Robust median filtering forensics by CNN-based multiple residuals learning," *IEEE Access*, vol. 7, pp. 120594–120602, 2019.
[43] M. Tadeusiewicz and S. Halgas, "A new approach to multiple soft fault diagnosis of analog BJT and CMOS circuits," *IEEE Trans. Instrum. Meas.*, vol. 64, no. 10, pp. 2688–2695, Oct. 2015.

**HUAHUI YANG** received the B.E. and M.E. degrees from the Ordnance Engineering College, in 2014 and 2016, respectively. He is currently pursuing the Ph.D. degree with the Missile Engineering Department, Army Engineering University, Shijiazhuang, China. His research interests include data-driven fault diagnosis and machine learning.

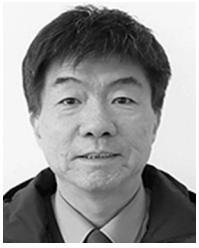

**CHEN MENG** received the Ph.D. degree from the Nanjing University of Science and Technology, Nanjing, China, in 2006. He is currently a Professor with the Missile Engineering Department, Army Engineering University, Shijiazhuang, China. His current research interests include automatic test systems (ATS), network for equipment support, and fault diagnosis.

**CHENG WANG** received the Ph.D. degree from the Ordnance Engineering College, Shiajiazhuang, China, in 2006. He is currently a Lecturer with the Missile Engineering Department, Army Engineering University. His research interests include automatic test systems (ATS), software architecture of ATS, and intelligent signal processing.